

# Design and Evaluation of a Nanoenhanced Anti-Infective Calcium Phosphate Bone Cements

Karthik K. Tappa, Udayabhanu M. Jammalamadaka and Dr. David K. Mills

**Abstract**— Post-operative complications due to infections are the most common problems that occur following dental and orthopedic implant surgeries and bone repair procedures. Preventing post-surgical infections is therefore a critical need that current polymethylmethacrylate (PMMA) bone cement fail to address. Calcium phosphate cements (CPCs) are unique in their ability to crystallize calcium and phosphate salts into hydroxyapatite (HA) and hence is naturally osteoconductive. Due to its low mechanical strength its use in implant fixation and bone repair is limited to non-load bearing applications. The present work describes a new and novel antibiotic-doped clay nanotube CPC composite with enhanced mechanical properties as well as sustained release properties.

## I. INTRODUCTION

Bone fractures are the most common injuries resulting from accidents, age and bone related diseases. When bone cannot regenerate itself bone grafts are implanted. An ideal bone graft should have the bioactive properties of osteogenesis (formation of new bone), osteoinduction (chemical process of inducing conversion of patient's osteoprogenitor cells into osteoblasts) and osteoconduction (providing a scaffold for cells to form new bone) [1]. These grafts must also set endothermically at body temperature and should have compressive strengths equal to or greater than bone. PMMA is widely used commercially available bone cement. This cement exhibits a high exothermic setting temperature ranging from 70°C-120°C during its implantation. A radiolucent fibrous tissue is observed at the bone/cement interface due to the release of toxic methylmethacrylate (MMA) monomers which damages surrounding tissue [2], [3]. In addition to this, PMMA cements lack elasticity and has a dense structure preventing bone from growing inside the cement. CPCs, on other hand, are osteoconductive and osteogenic [4]. They set endothermically at body temperature and have compressive strengths equal to or greater than bone. Low shrinkage, durability, dense or porous (depending on the site of injury), formability (ability to fill cavities of complex configurations) are additional positive qualities of CPCs [5].

Halloysite Nanotubes (HNTs) are two-layered aluminosilicate tubes that are found naturally as raw mineral deposits and are inexpensive commercially. When dehydrated 15-20 clay layers form a tubule making it hollow and capable of carrying drugs (Fig. 1). The inside of the lumen is positively charged and the external surface is negatively charged permitting additional functional modification of these surfaces. Due to physical properties

including nanosized lumens, high L/D ratio, low hydroxyl group density, cheap and abundant natural deposits, HNTs are being studied as a controlled or sustained release agent and for its ability to improve polymer mechanical performances and stability [6].

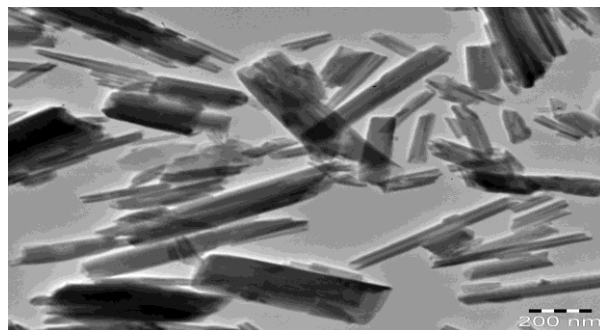


Figure 1. TEM image of HNTs.

Presently, the use of CPCs in regenerative medicine and orthopedic surgery is limited to only non-load bearing regions, i.e. cranioplasty. There is, therefore, a critical need for its application to load bearing sites due to its malleable nature and its osteogenic and osteoconductive capabilities. The aim of our work is to improve the material properties of CPCs and to obtain a sustained release drug profile by adding doped HNTs to the CPCs cement-laden mixture.

## II. MATERIALS AND METHODS

### A. Materials

Calcium phosphate dibasic anhydrous ( $\text{H}_2\text{CaO}_4\text{P}$ , DCPA),  $\beta$ -tri calcium phosphate ( $\text{Ca}_3\text{O}_8\text{P}_2$ ,  $\beta$ -TCP), calcium phosphate monobasic monohydrate ( $\text{H}_4\text{CaO}_8\text{P}_2 \cdot \text{H}_2\text{O}$ , MCPM), chitosan oligosaccharide lactate ( $(\text{C}_{12}\text{H}_{24}\text{N}_2\text{O}_9)_n$ ), chitosan (low molecular weight), polycaprolactone ( $\text{C}_6\text{H}_{10}\text{O}_2$ , PCL), calcium L-lactate ( $\text{C}_6\text{H}_{10}\text{CaO}_6 \cdot x\text{H}_2\text{O}$ ), HNTs ( $\text{H}_4\text{Al}_2\text{O}_9\text{Si}_2 \cdot 2\text{H}_2\text{O}$ ) were brought from Sigma-Aldrich, St. Louis, MO. Tetra calcium phosphate ( $\text{Ca}_4\text{O}_4\text{P}$ , TTCP) was ordered from CaP Biomaterials, E. Troy, WI. Cupric chloride ( $\text{CuCl}_2$ ) and calcium carbonate ( $\text{CaCO}_3$ ) were delivered from Nasco, Fort Atkinson, WI. Sodium phosphate dibasic ( $\text{Na}_2\text{HPO}_4$ ) was brought from Fisher Scientific Company, Waltham, MA.

### B. Preparation of samples

By using vacuum loading technique, HNTs were loaded with antibiotics (Gentamicin Sulfate (GS) and Neomycin Sulfate (NS) separately). Loaded HNTs were then mixed in different proportions with different compositions of calcium phosphate salts. All samples were hand mixed, using mortar

and pestle under ambient conditions (room temperature and atmospheric pressure) until a thick, moldable paste was formed. This paste was set into different shape molds for mechanical testing.

For compression testing cylindrical-shaped plastic molds with an inner diameter 6 mm and length 12 mm were used according to ISO standards no. 4104 [7]. Molds of inner dimensions 65 mm X 10 mm X 4 mm were prepared using paraffin wax in accordance with ASTM F417-78 standards [8]. For cell-culture techniques, CPCs 10 mm X 2 mm were made using steel molds.

### C. Material Characterization

Scanning electron microscope (SEM) was used to observe the surface properties of the CPC samples. Images were taken of the fracture interface of cement samples using a S4800 Field Emission SEM, HITACHI scanning electron microscope.

Compression and flexural tests were done using Admet Compression Machine with a cross-head velocity of 0.3 mm/min [9] and strongest formulation was selected for further development. To this formulation, different concentrations of HNTs were added and the effects of HNT concentration on mechanical properties of CPCs were tested.

### D. Cytological Assay

To assess osteoblasts grow and functionality on the well-formed CPCs, cells were cultured along with the CPC scaffolds and cellular response were assessed using different staining techniques including picosirius red, alcian blue and alkaline phosphatase (AP) activity.

### E. Drug Release Profile

Samples were collected from loaded HNTs and CPC scaffolds at regular intervals of time and were subjected to UV-Visible spectroscopy. For GS, indirect method of detection by ophthalaldehyde reagent was used and for detecting NS, copper chloride was used.

### F. Bacterial Culture

Confluent clinical grade strains of *Escherichia coli* and *Staphylococcus aureus* were cultured along with the CPC scaffolds at 37°C for 24 hours in an incubator. Inhibition zones were determined by measuring the diameter of the inhibited area at three points. The measured zone included the sample in the middle.

## III. RESULTS AND DISCUSSION

### A. Mechanical Properties

All formulations were subjected to compression testing. Three samples were tested for each formulation and the average was taken. The composition, TTCP (1.46 gm) and DCPA (0.54 gm) mixed in 10% w/v chitosan lactate, showed a cohesive nature and remained solid without disintegrating for several days after placement in simulated body fluid. This formulation was used for all further experiments.

When HNTs were added to this formulation and tested for any change in mechanical properties we noted an increase in compressive strength. This may be because of crack-tip blunting [10], process where a propagating crack is either

deflected, cracked or stopped because of solid particle obstruction. Different concentrations of HNTs in this formulation were subjected to compression testing, and the composition with 10% w/w of HNTs showed the highest compression resistance as compared with other formulations. CPC scaffolds with different L/D ratios of HNTs were also prepared and tested. There was no significant difference in mechanical properties when L/D ratios of HNTs were altered.

Specimens showed a gradual increase in load bearing capacity until 10% w/w of HNTs and started declining after further HNT addition. This may be due to uneven distribution of HNT particles resulting in cluster formation. Fig. 2 shows the compression pressure graph plotted against HNT concentration.

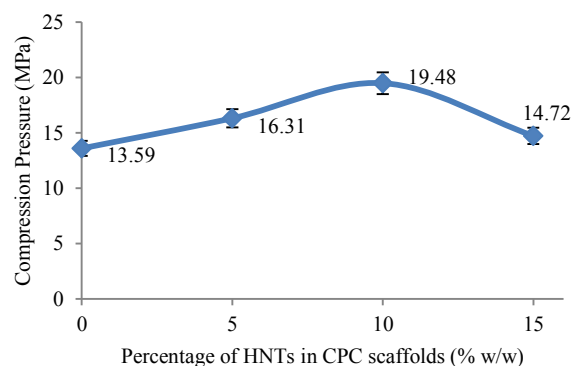


Figure 2. Graph plotted with percentage of HNTs (W/W %) against compression pressure (MPa).

Flexural strength of the scaffolds showed a slight increase when HNT concentration was increased from 5% to 10% w/w. Any addition of HNTs after 10% w/w yielded no increase in flexural strength (Fig. 3).

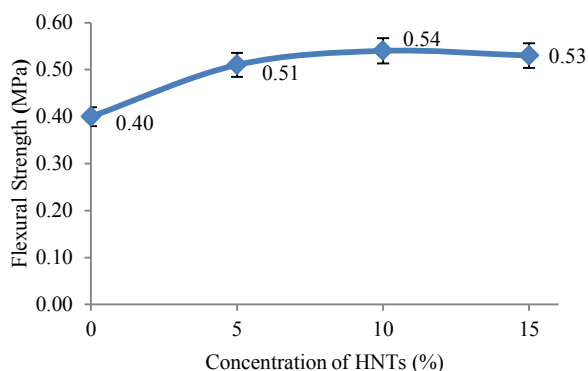


Figure 3. Graph showing variations in flexural strength with increase in HNT concentration.

### B. SEM

The SEM images (Fig. 4) clearly show an increase in surface roughness and porosity difference with addition of HNTs.

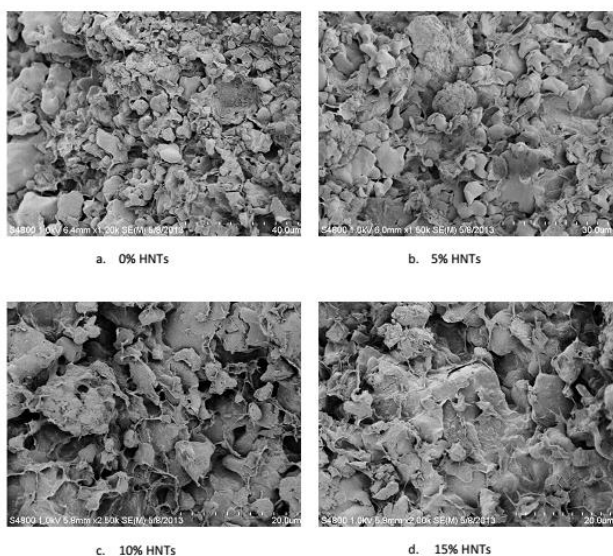


Figure 4. SEM images showing surface roughness of a. 0% HNTs, b. 5% HNTs, c. 10% HNTs and d. 15% HNTs in CPC scaffolds.

### C. Cytological Assay

Deep staining due to picosirius red was observed in the cell culture indicating the presence of collagen content (Fig. 5). Day 14 cultures were deeply stained than day 7, due to more collagen content.

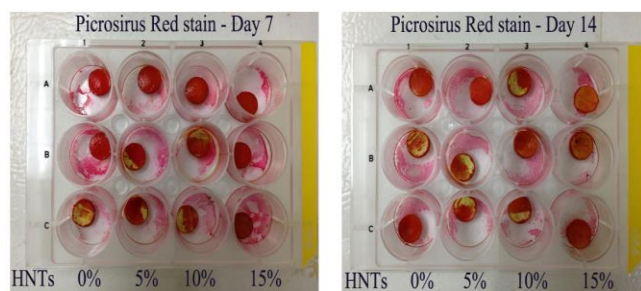


Figure 5. Histochemical analysis of collagen content using picosirius red.

Similar results were obtained for the detection of polysaccharides using alcian blue (Fig. 6). The scaffolds in the cell cultures were deeply stained suggesting the presence of acid mucopolysaccharides secretion.

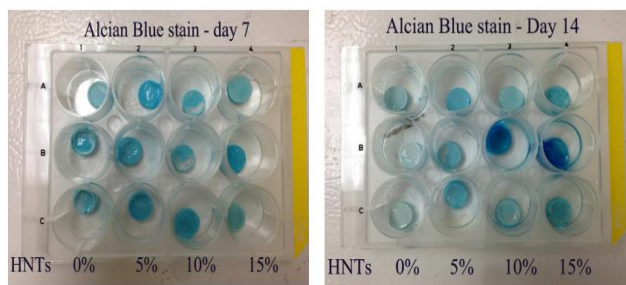


Figure 6. Histochemical analysis of acidic mucopolysaccharides using alcian blue.

AP activity was detected using BCIP/NBT as substrate. It was quantified and results were plotted as shown in Fig. 7. There was not much difference in the absorbance values on day 7 for 0%, 5% and 10% w/w HNT-CPC scaffolds. But an increase in activity for 15% w/w HNT concentration was observed. AP activity was more for day 14 for all the samples when compared to day 7, except for 15% w/w scaffolds. From these results we could say that prepared scaffolds are biocompatible.

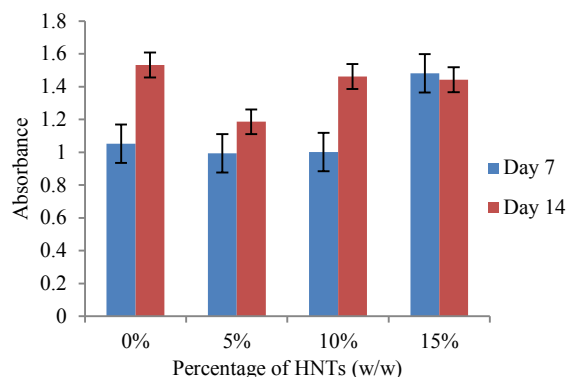


Figure 7. Comparison of absorbance values for samples collected at different concentrations of HNTs at day 7 and day 14.

### D. Drug Release Profile

The concentration of GS released from CPC scaffolds is shown in Fig. 8. Within 24 hours, 1.9 mg/ml of drug was released from HNTs and 0.9 mg/ml from the CPC scaffolds. This high release from scaffolds may be due to the burst release of the drug from HNTs on the surface of the scaffolds. Only a small amount was released thereafter, but it was steady and extended. Once the release amount reached 0.94 mg/ml by 48 hours, the release rate decreased. Scaffolds could only release 0.05 mg/ml from 48-144 hours, which was within the working concentration of the drug.

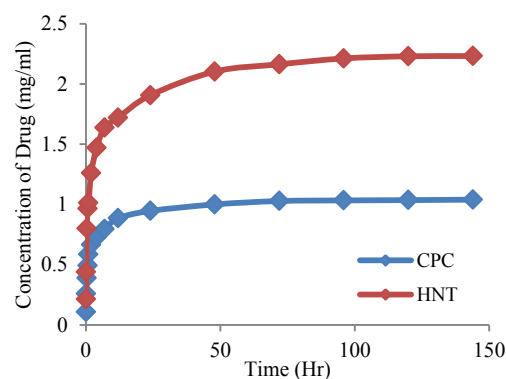


Figure 8. Graph showing concentrations of GS released from CPC scaffolds and HNTs at different time intervals.

The NS showed 1.04 mg/ml of drug release from CPC scaffolds within 24 hours. Whereas, HNTs alone showed 2.39 mg/ml release. A total of 1.12 mg/ml was released from scaffolds for a 7 day period as shown in the Fig. 9.

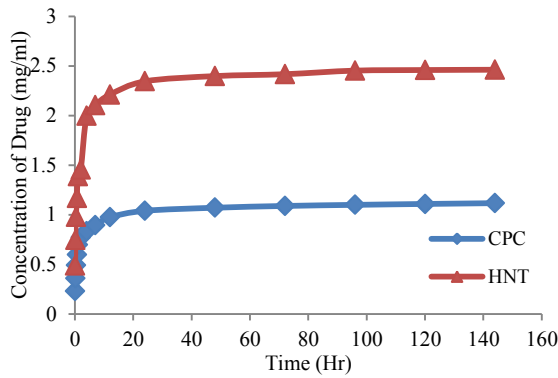


Figure 9. Graph showing concentrations of NS released for CPC scaffolds and HNTs at different time intervals.

Both antibiotic-release profiles demonstrate that after the first three to four days, the cement has released only a small amount of the drug (the amount was within working concentrations i.e., 60 $\mu$ g). The reason for this low release may be because the antibiotic inside the HNTs present on the surface of the scaffolds would have already emptied, and those HNTs entrapped inside the cement are not exposed to sampling liquid. The antibiotic release would have continued if the scaffolds were left to degrade.

#### E. Bacterial Culture

Hardened cement samples with different concentrations of HNTs were placed on the surface of LB-agar plates previously inoculated with *S. aureus* and *E. coli*. Zones of inhibition for both the strains and for both GS and NS were measured and a graph was plotted (Fig. 10).

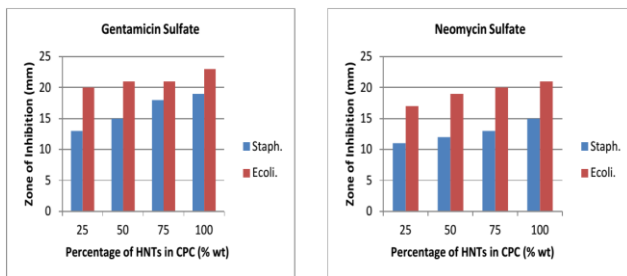


Figure 10. Illustration of the zone of inhibition around the CPC scaffolds with different HNT concentrations.

The scaffolds with 0% w/w HNTs did not show any inhibition, and all other samples showed inhibition zones ranging from 11 mm-23 mm diameter. With an increase in HNT concentrations, the diameter of inhibition was also increased. Interestingly, larger diameters were observed for *E. coli* when compared to *S. aureus* cultures. This might be because of *S. aureus* being a more resistant strain than *E. coli*.

#### IV. CONCLUSION

In this study it was shown that addition of HNTs to CPC increased compression and flexural strengths. SEM imaging of CPC scaffolds reveal that addition of HNTs in the mixture changed the morphology of the cement. They enhanced the

compact nature of the cement micro-particles, resulting in increased mechanical strength and surface roughness.

Cytological assays done on osteoblast cells with CPC-HNT scaffolds showed no deleterious effects on the cells, proving that HNTs do not cause harm *in vivo*. In addition to that, an increase in AP activity, collagen content and MPs content were recorded with the addition of HNTs. As the concentration of HNTs in CPC increased, surface roughness was increased providing them better chances for cell attachment and propagation resulting in enhanced osteoconductivity.

As HNTs are hollow and have high length/diameter ratio, they naturally have the ability to be loaded with substances and to yield a prolong release of them. Because of this property, when HNTs loaded with antibiotics are mixed with CPCs, they gave extended-release profiles. As the loaded HNTs are also present inside the scaffolds, we believe drug release would continue for several days when cement starts degrading to form bone. Zone of inhibition studies prove that the scaffolds were able to inhibit bacterial growth and provide an anti-infective field at the site of implantation.

#### REFERENCES

- [1] C. J. Damien and J. R. Parsons, "Bone graft and bone graft substitutes: a review of current technology and applications," *J. Appl. Biomater.*, vol. 2, no. 3, pp. 187–208, Jan. 1991.
- [2] J. E. Gough and S. Downes, "Osteoblast cell death on methacrylate polymers involves apoptosis," *J. Biomed. Mater. Res.*, vol. 57, no. 4, pp. 497–505, Dec. 2001.
- [3] E. Mitzner, P. Albertus, H. Maria, C. Mueller, and D. Berlin, "Material properties and *in vitro* biocompatibility of a newly developed bone cement," *Mater. Res.*, vol. 12, no. 4, pp. 447–454, 2009.
- [4] F. C. M. Driessens, J. Planell, M. G. Boltong, I. Khairoun, and M. P. Ginebra, "Osteotransductive bone cements," *J. Eng. Med.*, vol. 212, no. 6, pp. 427–435, Jun. 1998.
- [5] V. S. Komlev, I. V. Fadeeva, N. Gurin, L. I. Shvorneva, N. V. Bakunova, and S. M. Barinov, "New calcium phosphate cements based on tricalcium phosphate," *Dokl. Chem.*, vol. 437, no. 1, pp. 75–78, Apr. 2011.
- [6] M. Du, B. Guo, and D. Jia, "Newly emerging applications of halloysite nanotubes: a review," *Polym. Int.*, vol. 59, no. 5, pp. 574–582, 2010.
- [7] R. M. Khashaba, M. M. Moussa, D. J. Mettenberg, F. Rueggeberg, N. B. Chutkan, and J. L. Borke, "Polymeric-calcium phosphate cement composites-material properties: *in vitro* and *in vivo* investigations," *Int. J. Biomater.*, vol. 2, pp. 1–14, Jan. 2010.
- [8] S. M. Kurtz, M. L. Villarraga, K. Zhao, and A. A. Edidin, "Static and fatigue mechanical behavior of bone cement with elevated barium sulfate content for treatment of vertebral compression fractures," *Biomaterials*, vol. 26, no. 17, pp. 369–712, Jun. 2005.
- [9] K. Padois and F. Rodriguez, "Effects of chitosan addition to self-setting bone cement," *Biomed. Mater. Eng.*, vol. 17, no. 5, pp. 309–20, Jan. 2007.
- [10] A. H. Gomoll, W. Fitz, R. D. Scott, T. S. Thornhill, and A. Bellare, "Nanoparticulate fillers improve the mechanical strength of bone cement," *Acta Orthop.*, vol. 79, no. 3, pp. 421–7, Jun. 2008.